Sensors and Actuators B 210 (2015) 795–802

Contents lists available at ScienceDirect

Sensors and Actuators B: Chemical

journal homepage: www.elsevier.com/locate/snb

Mixed-potential type NH_3 sensor based on stabilized zirconia and $Ni_3V_2O_8$ sensing electrode

Fangmeng Liu, Ruize Sun, Yehui Guan, Xiaoyang Cheng, Han Zhang, Yingzhou Guan, Xishuang Liang*, Peng Sun, Geyu Lu**

State Key Laboratory on Integrated Optoelectronics, College of Electronic Science and Engineering, Jilin University, 2699 Qianjin Street, Changchun 130012, China

ARTICLE INFO

Article history:
Received 25 November 2014
Received in revised form 7 January 2015
Accepted 17 January 2015
Available online 25 January 2015

Keywords:
NH_3 sensor
Stabilized zirconia
$Ni_3V_2O_8$
Mixed potential

ABSTRACT

A mixed-potential type gas sensor using stabilized zirconia (YSZ) and a sensing electrode (SE) that consists of the new type composite oxide $Ni_3V_2O_8$ was developed for ammonia (NH_3) detection at elevated temperature, such as 650 °C. The $Ni_3V_2O_8$ materials were synthesized from $Ni(NO_3)_2{\cdot}6H_2O$ and NH_4VO_3 through the sol–gel method. $Ni_3V_2O_8$ sintered at different temperatures was also characterized using X-ray diffraction (XRD) and field-emission scanning electron microscopy (FESEM). The present study mainly focused on the effect of sintering temperature of SE materials (800 °C, 1000 °C, 1200 °C) on NH_3 sensing characteristics. Results showed that the $Ni_3V_2O_8$ calcined at 1000 °C exhibited the largest sensitivity in an NH_3 concentration range of 50–500 ppm at 650 °C. The response for the sensor attached with a $Ni_3V_2O_8$-SE sintered at 1000 °C to 100 ppm of NH_3 was approximately −62 mV. Moreover, ΔV almost varied linearly with the logarithm of NH_3 concentration in the range of 50–500 ppm, which the slope was −96 mV/decade. Furthermore, the present sensor also displayed small drifts over 30 days and cross-sensitivities in the presence of various interfering gases. The high-sensing characteristics of the sensor attached with a $Ni_3V_2O_8$-SE sintered at 1000 °C to NH_3 are explained in terms of the micro-structure of the SE and the high electrocatalytic activities induced by the beneficial effect of the interaction between the Ni and V two metal oxides.

© 2015 Elsevier B.V. All rights reserved.

1. Introduction

Diesel engines are widely applied in the fields of transportation, capital construction, industry, and power-generation, because of their high fuel efficiency, high power output, reliability, and low CO_2 emissions. However, their exhausts contain harmful air pollutants, especially NO_x. Therefore, an exhaust gas aftertreatment method for NO_x reduction must be developed urgently to meet the steadily increasing emission standards [1–4]. Among engine aftertreatment systems, selective catalytic reduction (SCR) that uses urea as reducing agent has been recognized as the most promising technology to eliminate the NO_x emissions from diesel vehicles [5,6]. In this system, a urea solution is injected into an exhaust line to react with the NO_x from combustion exhaust, as schematically presented in Fig. 1. To accurately control the amount of urea injected and to avoid NH_3 slips that aggravate air pollution problems, a powerful closed-loop feedback control system must be employed. This system utilizes an NH_3 exhaust gas sensor for on-board diagnosis (OBD). Furthermore, the NH_3 sensors to automobile exhausts must be tolerant of elevated temperatures because the long-term operation of a vehicle with a diesel engine reaches a high temperature under working conditions.

Thus far, various NH_3 sensors using different sensing materials, such as semiconducting oxide [7–17], zeolites [18], and organic compounds [19] have been proposed and reported by many researchers. However, such sensors are operated at lower temperatures and are unsuitable for the harsh exhaust gas environments. Fortunately, mixed-potential type NH_3 sensors based on stabilized zirconia (YSZ) and oxide electrodes have displayed potential under such harsh working conditions. Several researchers have reported the following related results: Miura et al. fabricated a planar YSZ-based sensor attached with a NiO/Au-SE that detects NH_3 at high temperatures. It exhibits excellent sensitivity and selectivity for the sensor to NH_3. The response (ΔV) of the sensor to 100 ppm NH_3 is approximately −34 mV, and the ΔV almost varies linearly with NH_3 concentration in the examined range of 20–100 ppm at

* Corresponding author. Tel.: +86 431 85168384; fax: +86 431 85167808.
** Corresponding author. Tel.: +86 431 85167808; fax: +86 431 85167808.
E-mail addresses: liangxs@jlu.edu.cn (X. Liang), lugy@jlu.edu.cn (G. Lu).

http://dx.doi.org/10.1016/j.snb.2015.01.043
0925-4005/© 2015 Elsevier B.V. All rights reserved.

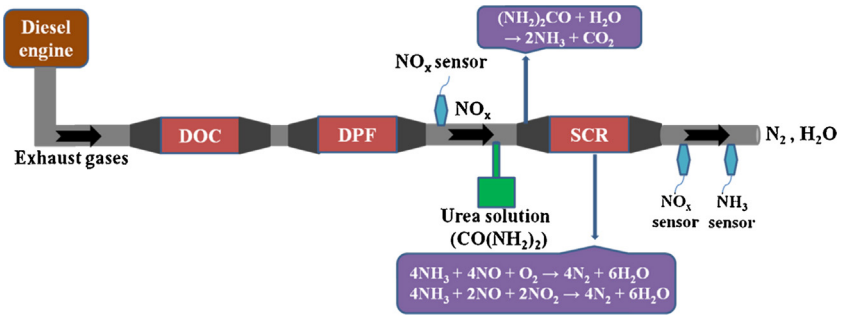

Fig. 1. Schematic view of exhaust gases aftertreatment system.

800 °C [20]. Moos et al. introduced a novel, selective, mixed potential NH_3 sensor that employs Au electrodes covered with a porous vanadia–tungstenia–titania-based SCR catalyst material. The sensor displays good cross-sensitivity and long-term stability to NH_3 in harsh exhaust environments and can detect very slight NH_3 slips at the downstream of an SCR catalyst [21]. Plashnitsa et al. reported that the YSZ-based planar sensor that utilizes a SE for spontaneously formed composites (nano-Au + nano-SiO_2) exhibits highly sensitive and selective NH_3 gas sensing properties at 700 °C [22]. Our group also presented an YSZ based NH_3 sensor using $CoWO_4$ as a SE. It displays fast response and recovery characteristics (not more than 5 s) and high sensitivity (−51 mV/decade) to NH_3 at 700 °C [23]. Thus, the design and preparation of novel oxide electrode materials with high electrochemical catalytic activity and excellent porosity is an important strategy to improve the sensing performance of mixed-potential type YSZ-based NH_3 sensor in terms of sensitivity, selectivity, and long-term stability.

Bimetallic oxide systems are of great interest in the design of new materials for catalysis, electrochemistry, and microelectronics. These systems are multiple-functionalities and exhibit prominent catalytic activity, selectivity, and stability over monometallic oxide materials [24,25]. NiO is among the most commonly used active materials in either pure or hydroxide form. It is well-known for its chemical stability as well as its catalytic and electrical properties. The application of NiO in electro-catalytic and electrochromic devices has been investigated, along with its use as SE material for gas sensors [26–28]. Vanadium oxide is an excellent catalyst for various catalytic reactions. In relation to the heterogeneous catalysis of vanadium oxides, redox property and surface acidity depend strongly on the additives or support oxide materials. For instance, the addition of Ni to V_2O_5 to form Ni–V–O compounds increases surface acidity with initial heat to 135 kJ/mol from 95 kJ/mol of V_2O_5 for the adsorption of NH_3. This finding indicates that such material possesses high surface acidity [29]. Moreover, the surface acidity of vanadium-based oxide can play an important role in the selective sensing of NH_3 [30,31]. The use of a suitably designed Ni/V composite that utilizes the beneficial effect of the interaction between the two metals to enhance electrocatalytic activities in combination with the performance of two materials can generate suitable SE material for NH_3 detection. As far as we know, a high temperature NH_3 sensor that employs the designed composite as SE material has not been developed.

Therefore, in this study, we investigate a new $Ni_3V_2O_8$ composite oxide material as SE for YSZ-based mixed-potential-type sensor, which can be used to detect NH_3 at elevated temperatures. To determine the sintering temperature factor that affects sensing properties, the effect of various sintering temperatures on sensing properties is studied. In addition, the detailed sensing characteristics and mechanism of this sensor are identified and discussed.

2. Experimental

2.1. Preparation and characterization of the $Ni_3V_2O_8$ SE material

The $Ni_3V_2O_8$ was prepared from nickel nitrate ($Ni(NO_3)_2{\cdot}6H_2O$), ammonium metavanadate (NH_4VO_3), glycine (Gly), and ethylene glycol (EG) by the sol–gel method. In a typical process, $Ni(NO_3)_2{\cdot}6H_2O$ and stoichiometric NH_4VO_3 (the molar ratio of Ni/V = 3:2) were dissolved in deionized water, respectively. Gly was added into the NH_4VO_3 solution (the molar ratio of Gly/V = 4:1) and stirred at 60 °C for 2 h to obtain a yellow transparent solution. EG and $Ni(NO_3)_2{\cdot}6H_2O$ solution were dropwise added into the mixture described above and then stirred at 90 °C until to a gel solution was obtained. The resultant solution was maintained at 80 °C for 12 h at electric vacuum drying oven. The precursor gel was then sintered at 400 °C, 600 °C, 800 °C, 1000 °C, and 1200 °C for 2 h in muffle furnace by a gradual increase of temperature.

X-ray diffraction (XRD) patterns of $Ni_3V_2O_8$ materials were measured by Rigaku wide-angle X-ray diffractometer (D/max rA, using Cu Kα radiation at wave length = 0.1541 nm). Field-emission scanning electron microscopy (FESEM) observations of surface morphology of the $Ni_3V_2O_8$-SE materials were obtained using a JEOL JSM-7500F microscope with an accelerating voltage of 15 kV.

2.2. Fabrication and measurement of the sensor

The sensor was fabricated using the YSZ plate (8 mol% Y_2O_3-doped, 2 mm × 2 mm square, 0.2 mm thickness, provided by Tosoh Corp., Japan). A point-shaped and a narrow stripe-shaped Pt electrode (reference electrode, RE) were formed on two ends of the YSZ plate using a commercial Pt paste (Sino-platinum Metals Co., Ltd.). The various $Ni_3V_2O_8$-SE materials sintered at 800 °C, 1000 °C, and 1200 °C were mixed with a minimum quantity of deionized water. The resultant paste was then applied on the point-shaped Pt to form stripe-shaped SE, followed by sintering at 800 °C for 2 h. The Pt heater formed on Al_2O_3 substrate was then attached to the YSZ plate by the inorganic adhesive, which provided the required heating temperature for the sensor. The gas sensing characteristics of the fabricated sensors were measured by a conventional static method [32,33]. Sample gases containing different NH_3 concentrations were obtained by diluting 10,000 ppm NH_3 with air. The electric potential difference (V) between the SE and the RE was measured with a digital electrometer (Rigol Technologies, Inc., DM3054, China) when the sensor was exposed to air or sample gas. The results obtained were recorded with a computer connected to the electrometer [34]. The current–voltage (polarization) curves of the sensor were carried out by means of the potentiodynamic method (CHI600C, Instrument corporation of Shanghai, China) using a two-electrode configuration in the base gas (air) and the sample gas (200 and 300 ppm NH_3 + air) at 650 °C.

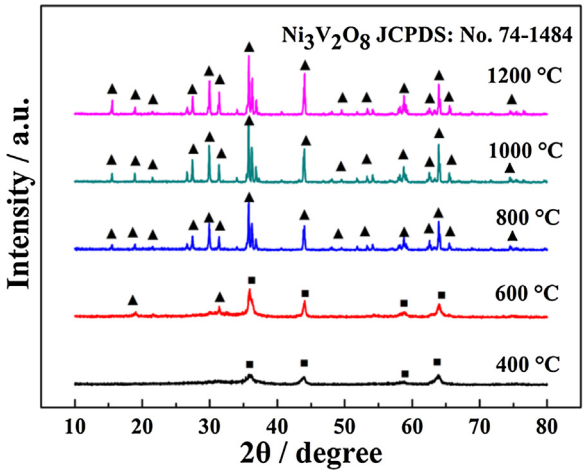

Fig. 2. XRD patterns of the prepared material sintered at different temperatures (■) NiO and (▲) $Ni_3V_2O_8$.

3. Results and discussion

Fig. 2 shows the XRD patterns of the prepared material sintered at different temperatures. The NiO with cubic structure is dominant when the dried gel was sintered at 400 °C. However, the peaks of $Ni_3V_2O_8$ were obviously strengthened, with the increasing of the sintering temperature. The diffraction peaks above 800 °C agreed well with the data of the Joint Committee on Power Diffraction Standards (JCPDS) (File No. 74-1484) regarding $Ni_3V_2O_8$ orthorhombic oxide. This indicated that the single phase of $Ni_3V_2O_8$ with orthorhombic structure was formed. The sharp diffraction peaks also suggested the good crystallinity of the as-prepared materials. The mean crystallite sizes of the $Ni_3V_2O_8$ samples sintered at 800 °C, 1000 °C, and 1200 °C were calculated by the Debye–Scherrer equation, which were around 30, 65, and 84 nm, respectively.

The SEM images of $Ni_3V_2O_8$-SEs sintered at different temperatures (800 °C, 1000 °C, and 1200 °C) are shown in Fig. 3. The particles were gradually enlarged and the porosity of the morphology was enhanced with the increase in calcined temperature. Additionally, the diameter of the small microparticles of the $Ni_3V_2O_8$ sintered at 1000 °C was roughly 0.2–2 μm. That of the bulk particles was approximately 2–6 μm.

To research the effect of sintering temperature on sensing property, the sensors attached with $Ni_3V_2O_8$ calcined at different temperatures (800 °C, 1000 °C, and 1200 °C) were fabricated. Fig. 4 shows the dependence of the ΔV on the logarithm of NH_3 concentrations for the sensors using $Ni_3V_2O_8$-SEs calcined at 800 °C, 1000 °C, and 1200 °C in the range of 50–500 ppm at operating temperature of 650 °C. Three sensors based on different sintering temperatures exhibited good sensitivity to NH_3 at 650 °C. Among these sensors, the one using the $Ni_3V_2O_8$ sintered at 1000 °C displayed the largest slope (−96 mV/decade). This result may be attributed to several reasons. When the sensor was exposed to the NH_3 atmosphere, two main processes took place on the SE. Firstly, the NH_3 penetrated the electrode layer to disperse on the triple-phase-boundary (TPB). Secondly, the cathodic (1) and anodic (2) reactions can occur simultaneously and form a local cell at the TPB of the SE. When the rates of the cathodic and anodic reactions are equal, the sensing electrode potential is mixed potential.

$$\text{Cathodic}: \ 1/2O_2 + 2e^- \rightarrow O^{2-} \quad (1)$$

$$\text{Anodic}: \ 2/3NH_3 + O^{2-} \rightarrow 1/3N_2 + H_2O + 2e^- \quad (2)$$

The mixed potential intensity is related to the degree of anodic reaction (2), and the faster the anodic reaction (2), the higher the sensitivity. Several methods can be employed to promote reaction (2): (1) increasing the reaction of NH_3 concentration; (2) enlarging the area of TPB; (3) improving the electrochemical catalytic activity of SE.

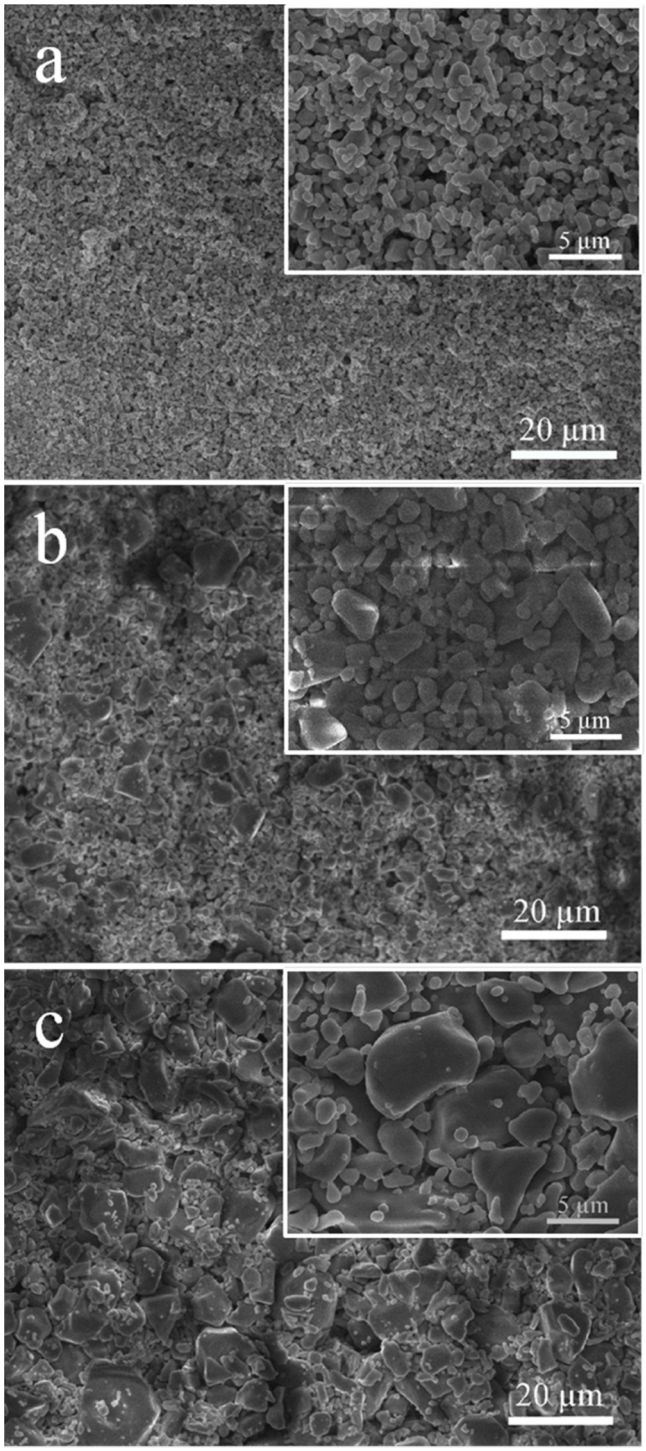

Fig. 3. SEM images of $Ni_3V_2O_8$-SEs sintered at different temperatures: (a) 800 °C, (b) 1000 °C, and (c) 1200 °C.

As indicated in Fig. 3, the porosity of the SE materials prepared at different temperatures was increased with the increasing of the sintering temperature. The tunnels formed by large particles could facilitate NH_3 to diffuse easily into the SE layers and reduced the NH_3 consumption ($4NH_3 + 3O_2 \rightarrow 2N_2 + 6H_2O$) caused by the high chemically catalytic activity of $Ni_3V_2O_8$ in the process of gas

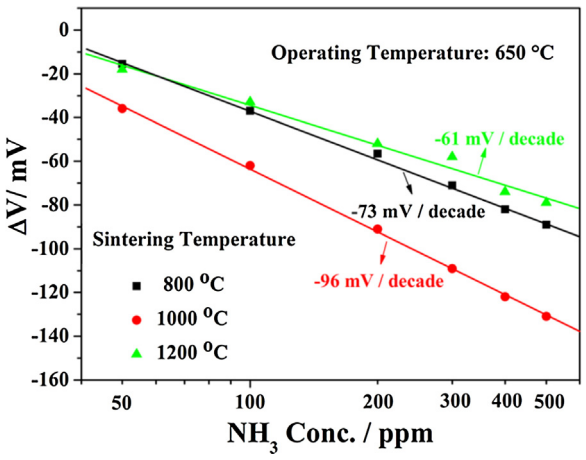

Fig. 4. Dependence of ΔV on the logarithm of NH_3 concentrations for the sensors using $Ni_3V_2O_8$-SEs calcined at 800 °C, 1000 °C, and 1200 °C in the range of 50–500 ppm at 650 °C.

diffusion. As a result, the increased amount of NH_3 reached the TPB and participated in the electrochemical reactions. In this case, the higher calcined temperature induced the higher sensitivity. Nonetheless, the particles of $Ni_3V_2O_8$ became too large when the sintering temperature was too high, and the electrochemical activity of the $Ni_3V_2O_8$ decreased obviously. Therefore, the sensitivity of the sensor with $Ni_3V_2O_8$ sintered at 1200 °C decreased.

The electrochemical catalytic activity of the $Ni_3V_2O_8$ sintered at 1000 °C could be higher than those of the two samples sintered at the other temperatures, and result in the fastest reaction (2). To examine the electrochemical catalytic properties of the sensing materials sintered at different temperatures, the modified polarization curves in air and 300 ppm NH_3 for the sensor attached with $Ni_3V_2O_8$-SEs sintered at 800 °C, 1000 °C, and 1200 °C were measured and shown in Fig. 5 [35,36]. The sensor attached with $Ni_3V_2O_8$-SE sintered at 1000 °C exhibited the highest anodic activity, by comparing the anodic polarization curves of the sensors using $Ni_3V_2O_8$-SEs sintered at different temperatures. Aside from its higher electrochemically catalytic activity, as expressed, the better porosity of the $Ni_3V_2O_8$-SE sintered at 1000 °C also played an important role in improving the sensing performance to NH_3. Additionally, the mixed potential can be estimated from the intersection of the anodic and cathodic polarization curves. Based on the comparison of the mixed potential estimated values and the potential difference values experimentally observed for the fabricated devices, in Table 1, the estimated values are in close proximity

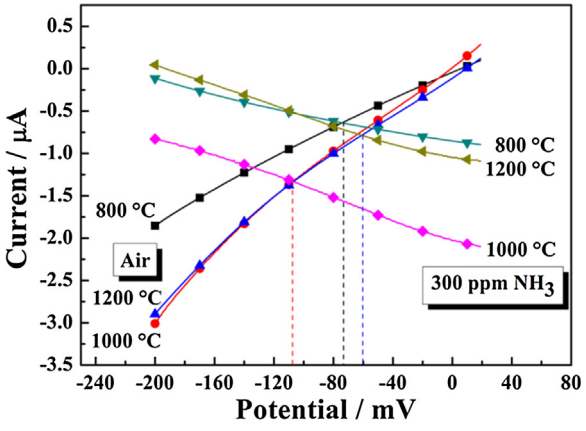

Fig. 5. Modified polarization curves in air and 300 ppm NH_3 for the sensor attached with $Ni_3V_2O_8$-SE sintered at 800 °C, 1000 °C, and 1200 °C.

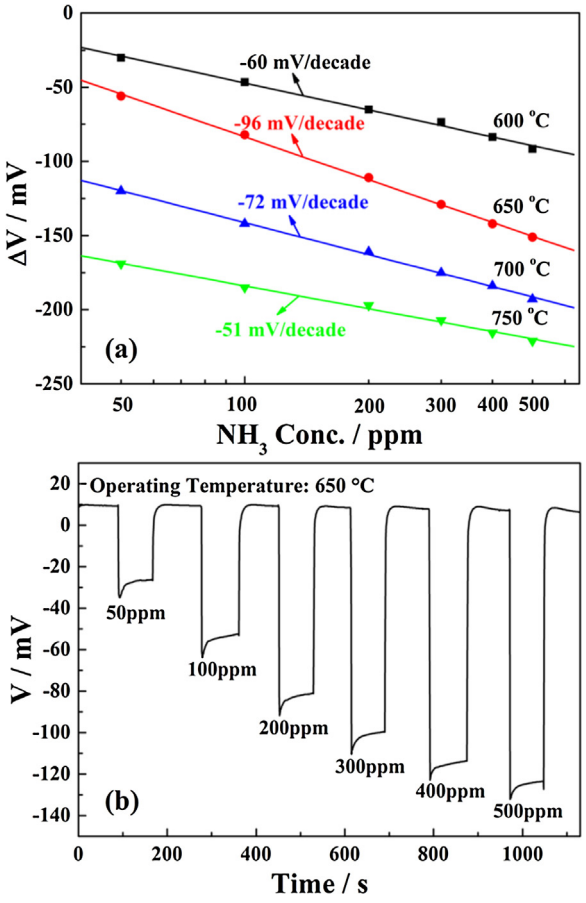

Fig. 6. (a) Dependence of ΔV on NH_3 concentrations for the sensors attached with $Ni_3V_2O_8$-SE sintered at 1000 °C at different operating temperatures; (b) response transients curve for the YSZ-based sensor attached with $Ni_3V_2O_8$-SE sintered at 1000 °C toward different concentrations of NH_3 in the range of 50–500 ppm at 650 °C.

to those observed values for 300 ppm NH_3. These coincidences indicate that the present sensors conform to the mixed-potential mechanism [37–39].

Among the $Ni_3V_2O_8$ sintered at different temperatures, the $Ni_3V_2O_8$ sensing material calcined at 1000 °C showed the largest sensitivity. Therefore, we paid much attention to the sensor based on $Ni_3V_2O_8$-SE sintered at 1000 °C. As known very well, the sensitivity of the sensor depended strongly on the operation temperatures. The dependence of the ΔV on NH_3 concentrations for the sensors attached with $Ni_3V_2O_8$-SE sintered at 1000 °C at different operating temperatures are shown in Fig. 6(a). The NH_3 sensitivity was linearly dependent on the logarithm of NH_3 concentration in the examined range of 50–500 ppm at each operating temperature, which is usually observed in mixed-potential type sensors. The slope tended to increase initially below 650 °C with the increasing of the operating temperature. At 650 °C, a maximum value, with a slope of −96 mV/decade was achieved. Above 650 °C, the slope tended to decrease. This result may be related to the amount of the NH_3 diffused through the $Ni_3V_2O_8$-SE to the TPB. Moreover, the electrochemical reaction happening at TPB can be affected by operating temperature and the occurrence of the electrochemical reaction at TPB needed definite activation energy [40]. The electrochemical reaction did not gain enough activation energy at below 650 °C, thus, the sensitivity of the sensor to NH_3 increased with the increasing of temperature. However, the desorption process of NH_3 exhibited dominant at above 650 °C, and the amount of NH_3 adsorbed on the SE became less and less along with the increasing temperature. Hence, the sensitivity of the sensor to NH_3 decreased

Table 1
Comparison of the mixed potential estimated and the potential difference value observed for the sensors using $Ni_3V_2O_8$-SEs sintered at 800 °C, 1000 °C, and 1200 °C.

Sensors	NH_3 conc. (ppm)	Mixed potential (estimated) (mV)	Potential difference value (observed) (mV)
$Ni_3V_2O_8$ (800 °C)-SE	300	−73	−71
$Ni_3V_2O_8$ (1000 °C)-SE	300	−108	−109
$Ni_3V_2O_8$ (1200 °C)-SE	300	−60	−58

Table 2
Comparison of the sensing performance of the present sensor and that of devices reported in literatures.

Material	Operating temperature (°C)	NH_3 concentration (ppm)	Sensor response (mV)	Sensitivity (slope) (mV/decade)	Reference
NiO/Au	800	100	−34	4	[20]
$CuNb_2O_6$	300	500	56	–	[41]
Porous Cr_2O_3	350	500	−110	−89	[32]
$CoWO_4$	700	100	−8	−51	[23]
Pt-WO_3	350	4000	45	–	[42]
Bi_2O_3	600	500	68.2	24	[43]
$Ni_3V_2O_8$	650	100	−62	−96	This work

with further increases in operating temperature. Consequently, the optimal operating temperature for the present sensor was considered to be 650 °C. Additionally, from Fig. 6(b), the ΔV of the sensor changed quickly upon switching on- and off-NH_3 at 650 °C, and reached the steady-state potential difference value in a short time. Among the range of measured concentrations, the response and recovery rates are fast. The 90% response and recovery times of the sensor to 500 ppm NH_3 were approximately 2 and 10 s, respectively. The response of the sensor to 100 ppm NH_3 was still as large as −62 mV. The comparison of the NH_3 sensing performances for the present fabricated sensor and that reported in literature is presented in Table 2. The present sensor displayed better performances than previously reported devices. It displayed the fast response and recovery rates, as well as high sensitivity to NH_3, at such high operating temperature. This performance is vital to on-board detection for controlling the NH_3 concentrations fast and accurately. Additionally, in Fig. 6(b), for the peak behavior at the beginning, there may be the following reasons: firstly, may be because of the effect of environmental factor in the process of switching gases. Secondly, the sensor was switched on NH_3, the gas penetrated fast the sensing electrode layer to disperse on the TPB. In the early, the rate of the anodic reaction is higher than that of the cathodic reaction. Therefore, the response of the sensor shows a peak at the beginning. When the rates of the above two electrochemical reactions are equal, the potential tends to attain the stable value. However, further study on the sensing performance in the future work is yet to be done for understanding the electro-chemical behavior very well.

The continuous response–recovery transients of the sensor using $Ni_3V_2O_8$-SE sintered at 1000 °C switching on- and off-200 ppm NH_3 at 650 °C had been measured as shown in Fig. 7. It was clearly seen that the potential difference response to 200 ppm NH_3 and air was effectively reproduced in the examined nine-time cycles, which was confirmed that the sensor exhibited good repeatability.

Moreover, in order to investigate the practical applicability for NH_3 detection, the selectivity and long-term stability measurements of the fabricated device were carried out. Fig. 8 shows the cross-sensitivities of the sensor attached with $Ni_3V_2O_8$-SE sintered at 1000 °C to various gases, such as NO_2, NO, H_2, CH_4, CO, Cl_2, C_2H_4 and C_7H_8 at 650 °C. Fig. 8 suggested that the sensor exhibited larger sensitivity to 200 ppm NH_3 than the other gases. Furthermore, due to the coexistence of NH_3 in conjunction with NO_2 in exhaust gas, the sensitivity of the sensor to the mixture of gases (200 ppm NH_3 + 200 ppm NO_2) was obtained. Based on the comparison of the response value to mixture gases and 200 ppm NH_3 for fabricated sensor, there was relatively small change. It demonstrates that the

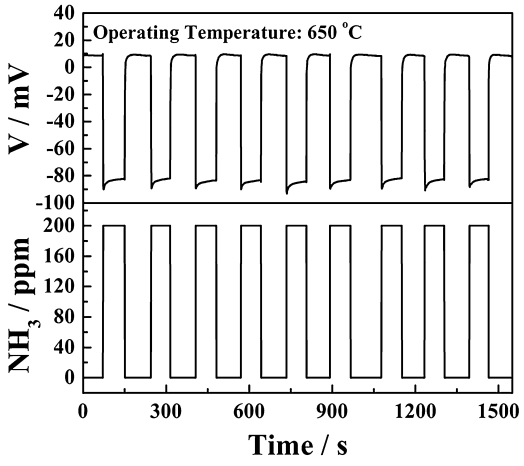

Fig. 7. Continuous response–recovery transients of the sensor using $Ni_3V_2O_8$-SE sintered at 1000 °C switching on- and off-200 ppm NH_3 at 650 °C.

sensor attached with $Ni_3V_2O_8$-SE sintered at 1000 °C has excellent selectivity to NH_3 against the other interfering gases.

The long-term stability of the sensor attached with $Ni_3V_2O_8$-SE sintered at 1000 °C to 100, 200, and 300 ppm NH_3 was measured at 650 °C, as illustrated in Fig. 9(a). The amplitude of the ΔV for the sensor using $Ni_3V_2O_8$-SE sintered at 1000 °C changed slightly to the same NH_3 concentration during the 30 days measurement

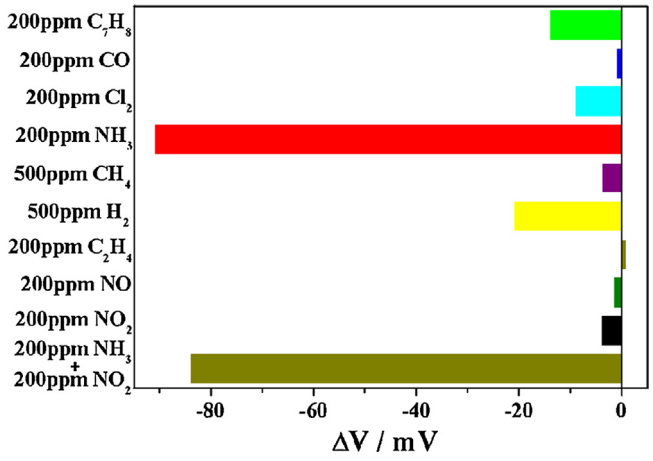

Fig. 8. Cross-sensitivities for the sensor attached with $Ni_3V_2O_8$-SE sintered at 1000 °C to various gases at 650 °C.

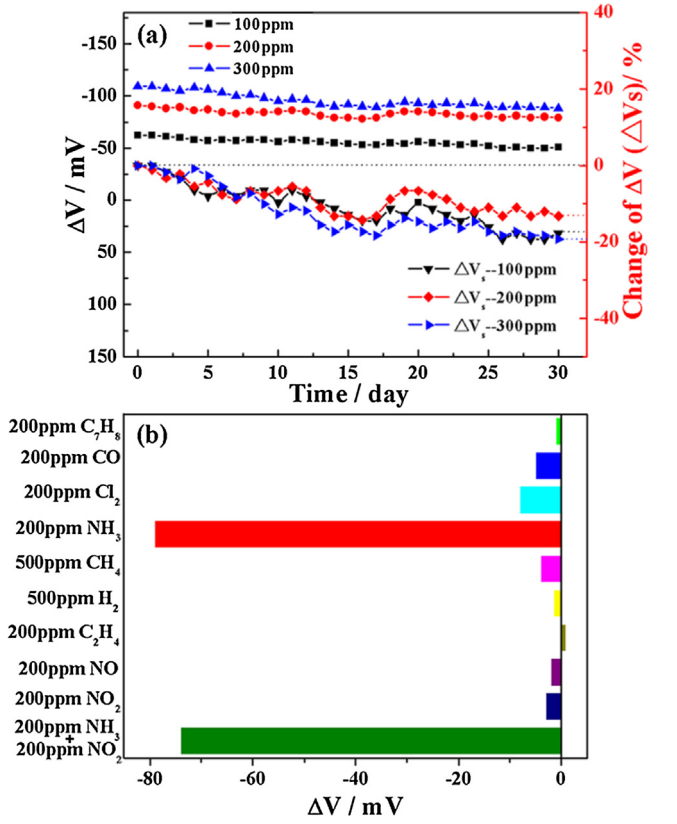

Fig. 9. (a) Long-term stability of the sensor attached with $Ni_3V_2O_8$-SE sintered at 1000 °C to 100, 200, and 300 ppm NH_3 at 650 °C; (b) cross-sensitivities of the sensor attached with $Ni_3V_2O_8$-SE sintered at 1000 °C to various gases measured on the 30th day of examination at 650 °C.

period. In order to further illustrate exactly the change amplitude of the ΔV with time, the change of the ΔV (ΔV_S) for the sensor is given by $\Delta V_S = [(\Delta V_n - \Delta V_0)/\Delta V_0 \times 100\%]$, where ΔV_n and ΔV_0 denote the ΔV of the sensor on the n and 0 day, respectively. The results show that the ΔV_S to 100, 200, and 300 ppm NH_3 on the 30th day are −17.7%, −13.2%, and −19.3%, respectively. Therefore, the present sensor showed better stability. Fig. 9(b) shows the cross-sensitivities of the sensor attached with $Ni_3V_2O_8$-SE sintered at 1000 °C to various gases measured on the 30th day of examination at 650 °C. It was found that the sensor still exhibited excellent sensitivity to NH_3 and selectivity to various interfering gases even at elevated temperature for a long term that after 30 days.

As mentioned previously, the sensing behavior of the present sensor exhibits the excellent linear relationship between potential difference and logarithm of the NH_3 concentration, which can be explained by the mixed-potential mechanism [44–46]. This sensor forms the following electrochemical cell.

In air: air, $Ni_3V_2O_8$/YSZ/Pt, air
In sample gas: NH_3 (+air), $Ni_3V_2O_8$/YSZ/Pt, NH_3 (+air)

The difference of the sensing and reference electrode potentials was measured as the sensing signal. Moreover, the potential response of the sensor to NH_3 in air can be studied quantitatively, as reported in [47–49]. The electric current densities for electrochemical reactions (1) and (2) can be described as following equations.

$$i_{NH_3} = i^0_{NH_3} \exp\left[\frac{2\alpha_1 F(V - V^0_{NH_3})}{RT}\right] \quad (3)$$

$$i_{O_2} = i^0_{O_2} \exp\left[\frac{-2\alpha_2 F(V - V^0_{O_2})}{RT}\right] \quad (4)$$

where V is the electrode potential; F is the Faraday constant; V^0 is the electrode potential at equilibrium; i^0 and α represent the exchange current density and transfer coefficient, respectively; R is the gas constant and T is the temperature. We hypothesize that i^0 abides by the following kinetic equations.

$$i^0_{NH_3} = B_1 C^m_{NH_3} \quad (5)$$

$$i^0_{O_2} = -B_2 C^n_{O_2} \quad (6)$$

where B_1, B_2, m, and n are constants, C_{NH_3} and C_{O_2} represent the concentration of NH_3 and O_2, respectively, and $i^0_{NH_3}$ and $i^0_{O_2}$ are values with opposite signs. When the cathodic and anodic electrochemical reactions reach equilibrium, $i_{NH_3} + i_{O_2} = 0$ is established, and the mixed potential is represented by $V_M(\Delta V)$:

$$V_M = V_0 + mA \ln C_{O_2} - nA \ln C_{NH_3} \quad (7)$$

Here,

$$V_0 = \frac{RT}{(2\alpha_1 + 2\alpha_2)F} \ln \frac{B_2}{B_1} + \frac{\alpha_1 V^0_{NH_3} + \alpha_2 V^0_{O_2}}{\alpha_1 + \alpha_2} \quad (8)$$

$$A = \frac{RT}{(2\alpha_1 + 2\alpha_2)F} \quad (9)$$

When Eq. (7) is combined with Eq. (8), the concentrations of O_2 and NH_3 are fixed, the mixed potential is equal to the electrode potential at equilibrium. When C_{O_2} value is a constant, Eq. (7) is simplified to the following equation:

$$V_M = V_0 - nA \ln C_{NH_3} \quad (10)$$

From Eq. (10), it is clearly that V_M varies linearly to the logarithm of NH_3 concentration ($\ln C_{NH_3}$) under the fixed C_{O_2} value, which has been demonstrated in Fig. 4 very well. Such theoretical analysis indicates that the NH_3 sensor using YSZ and a $Ni_3V_2O_8$-SE obeyed the mixed potential mechanism.

4. Conclusion

In summary, a new SE material ($Ni_3V_2O_8$) was prepared using the sol–gel method. Mixed-potential type sensors based on YSZ-plate and $Ni_3V_2O_8$-SE calcined at different temperatures (800 °C, 1000 °C, and 1200 °C) were designed to detect NH_3 at elevated temperatures. The result indicated that the sensor using $Ni_3V_2O_8$ calcined at 1000 °C exhibits the largest sensitivity (−96 mV/decade) to NH_3 at 650 °C. The response values for the fabricated device to 100 and 500 ppm NH_3 were −62 and −131 mV at 650 °C, respectively. The present sensor also showed better repeatability, long-term stability, and selectivity against various interfering gases. In addition, the sensing mechanism of the NH_3 sensor involved mixed potential on the basis of the measurement of the polarization curves was further demonstrated. Given these excellent sensing characteristics, the sensor has potential application value in the OBD system of vehicle exhaust gas.

Acknowledgements

This work is supported by Application and Basic Research of Jilin Province (20130102010JC), the National Natural Science Foundation of China (Nos. 61134010, 61327804, 61374218, 61377058 and 61473132), Program for Chang Jiang Scholars and Innovative Research Team in University (No. IRT13018) and National High-Tech Research and Development Program of China (863 Program, Nos. 2013AA030902 and 2014AA06A505).

References

[1] D. Chatterjee, P. Kočí, V. Schmeißer, M. Marek, M. Weibel, B. Krutzsch, Modelling of a combined NO_x storage and NH_3-SCR catalytic system for diesel exhaust gas aftertreatment, Catal. Today 151 (2010) 395–409.

[2] P. Forzatti, L. Lietti, E. Tronconi, Nitrogen oxides removal, in: I.T. Horvath (Ed.), Industrial Encyclopedia of Catalysis, 2002.

[3] A. Güthenke, D. Chatterjee, M. Weibel, B. Krutzsch, P. Kočí, M. Marek, I. Nova, E. Tronconi, Current status of modelling lean exhaust gas aftertreatment catalysts, Adv. Chem. Eng. 33 (2007) 103–211.

[4] R. Moos, D. Schönauer, Recent developments in the field of automotive exhaust gas ammonia sensing, Sens. Lett. 6 (2008) 808–811.

[5] M. Koebel, M. Elsener, T. Marti, NO_x-reduction in diesel exhaust gas with urea and selective catalytic reduction, Combust. Sci. Technol. 121 (1996) 85–102.

[6] M. Koebel, M. Elsener, M. Kleemann, Urea-SCR: a promising technique to reduce NO_x emissions from automotive diesel engines, Catal. Today 59 (2000) 335–345.

[7] C.N. Xu, N. Miura, Y. Ishida, K. Matsuda, N. Yamazoe, Selective detection of NH_3 over NO in combustion exhausts by using Au and MoO_3 doubly promoted WO_3 element, Sens. Actuators B: Chem. 65 (2000) 163–165.

[8] A.K. Prasad, D.J. Kubinski, P.I. Gouma, Comparison of sol–gel and ion beam deposited MoO_3 thin film gas sensors for selective ammonia detection, Sens. Actuators B: Chem. 93 (2003) 25–30.

[9] A.R. Raju, C.N.R. Rao, MoO_3/TiO_2 and Bi_2MoO_6 as ammonia sensors, Sens. Actuators B: Chem. 21 (1994) 23–26.

[10] D. Mutschall, K. Holzner, E. Obermeier, Sputtered molybdenum oxide thin films for NH_3 detection, Sens. Actuators B: Chem. 35–36 (1996) 320–324.

[11] A. Teeramongkonrasmee, M. Sriyudthsak, Methanol and ammonia sensing characteristics of sol–gel derived thin film gas sensor, Sens. Actuators B: Chem. 66 (2000) 256–259.

[12] V. Romanovskaya, M. Ivanovskaya, P. Bogdanov, A study of sensing properties of Pt- and Au-loaded In_2O_3 ceramics, Sens. Actuators B: Chem. 56 (1999) 31–36.

[13] P.F. Guo, H.B. Pan, Selectivity of Ti-doped In_2O_3 ceramics as an ammonia sensor, Sens. Actuators B: Chem. 114 (2006) 762–767.

[14] K. Shimizu, I. Chinzei, H. Nishiyama, S. Kakimoto, S. Sugaya, W. Matsutani, A. Satsuma, Doped-vanadium oxides as sensing materials for high temperature operative selective ammonia gas sensors, Sens. Actuators B: Chem. 141 (2009) 410–416.

[15] P. Ivanov, J. Hubalek, K. Malysz, J. Prášek, X. Vilanova, E. Llobet, X. Correig, A route toward more selective and less humidity sensitive screen-printed SnO_2 and WO_3 gas sensitive layers, Sens. Actuators B: Chem. 100 (2004) 221–227.

[16] M. Aslam, V.A. Chaudhary, I.S. Mulla, S.R. Sainkar, A.B. Mandale, A.A. Belhekar, K. Vijayamohanan, A highly selective ammonia gas sensor using surface-ruthenated zinc oxide, Sens. Actuators B: Chem. 75 (1999) 162–167.

[17] E. Llobet, G. Molas, P. Molinàs, J. Calderer, X. Vilanova, J. Brezmes, J.E. Sueiras, X. Correig, Fabrication of highly selective tungsten oxide ammonia sensors, J. Electrochem. Soc. 147 (2000) 776–779.

[18] R. Moos, R. Müller, C. Plog, A. Knezevic, H. Leye, E. Irion, T. Braun, K.J. Marquardt, K. Binder, Selective ammonia exhaust gas sensor for automotive applications, Sens. Actuators B: Chem. 83 (2002) 181–189.

[19] X. Chen, D.M. Li, S.F. Liang, S. Zhan, M. Liu, Gas sensing properties of surface acoustic wave NH_3 gas sensor based on Pt doped polypyrrole sensitive film, Sens. Actuators B: Chem. 177 (2013) 364–369.

[20] P. Elumalai, V.V. Plashnitsa, Y. Fujio, N. Miura, Stabilized zirconia-based sensor attached with NiO/Au sensing electrode aiming for highly selective detection of ammonia in automobile exhausts, Electrochem. Solid State Lett. 11 (2008) J79–J81.

[21] D. Schönauer, K. Wiesner, M. Fleischer, R. Moos, Selective mixed potential ammonia exhaust gas sensor, Sens. Actuators B: Chem. 140 (2009) 585–590.

[22] V.V. Plashnitsa, P. Elumalai, Y. Fujio, T. Kawaguchi, N. Miura, Spontaneous gradual accumulation of hexagonally-aligned nano-silica on gold nanoparticles embedded in stabilized zirconia: a pathway from catalytic to NH_3-sensing performance, Nanoscale 3 (2011) 2286–2293.

[23] Q. Diao, F.S. Yang, C.G. Yin, J.G. Li, S.Q. Yang, X.S. Liang, G.Y. Lu, Ammonia sensors based on stabilized zirconia and $CoWO_4$ sensing electrode, Solid State Ionics 225 (2012) 328–331.

[24] J.A. Rodriguez, Physical and chemical properties of bimetallic surfaces, Surf. Sci. Rep. 24 (1996) 223–287.

[25] N.M. Markovic, P.N. Ross Jr., Surface science studies of model fuel cell electrocatalysts, Surf. Sci. Rep. 45 (2002) 117–229.

[26] S. Zafeiratos, F.E. Paloukis, M.M. Jaksic, S.G. Neophytides, Thermal stability of electrodeposited nickel on vanadium: evidence for oxygen diffusion and intermetallic phase formation, Surf. Sci. 552 (2004) 215–228.

[27] T. Sato, V.V. Plashnitsa, M. Utiyama, N. Miura, Potentiometric YSZ-based sensor using NiO sensing electrode aiming at detection of volatile organic compounds (VOCs) in air environment, Electrochem. Commun. 12 (2010) 524–526.

[28] J. Park, B.Y. Yoon, C.O. Parka, W.-J. Lee, C.B. Lee, Sensing behavior and mechanism of mixed potential NO_x sensors using NiO, NiO(+YSZ) and CuO oxide electrodes, Sens. Actuators B 135 (2009) 516–523.

[29] C. Balamurugan, D.-W. Lee, A selective NH_3 gas sensor based on mesoporous p-type NiV_2O_6 semiconducting nanorods synthesized using solution method, Sens. Actuators B 192 (2014) 414–422.

[30] P. Gronchi, E. Tempesti, C. Mazzocchia, Metal dispersion dependent selectivities for syngas conversion to ethanol on V_2O_3 supported rhodium, Appl. Catal. A: Gen. 120 (1994) 115–126.

[31] A. Baiker, P. Dollenmeier, M. Glinski, A. Reller, Selective catalytic reduction of nitric oxide with ammonia. II. Monolayers of vanadia immobilized on titania–silica mixed gels, Appl. Catal. 35 (1987) 365–380.

[32] X. Niu, W. Du, W. Du, Preparation and gas sensing properties of ZnM_2O_4 (M = Fe, Co, Cr), Sens. Actuators B: Chem. 99 (2004) 405–409.

[33] Q. Diao, C.G. Yin, Y.Z. Guan, X.S. Liang, S. Wang, Y.W. Liu, Y.F. Hu, H. Chen, G.Y. Lu, The effects of sintering temperature of $MnCr_2O_4$ nanocomposite on the NO_2 sensing property for YSZ-based potentiometric sensor, Sens. Actuators B: Chem. 177 (2013) 397–403.

[34] H. Zhang, X.Y. Cheng, R.Z. Sun, Y.Z. Guan, Y.W. Liu, C.G. Yin, X.S. Liang, G.Y. Lu, Enhanced chlorine sensing performance of the sensor based NAISCON and Cr-series spinel-type oxide electrode with aging treatment, Sens. Actuators B: Chem. 198 (2014) 26–32.

[35] G.Y. Lu, N. Miura, N. Yamazoe, High-temperature hydrogen sensor based on stabilized zirconia and a metal oxide electrode, Sens. Actuators B: Chem. 35–36 (1996) 130–135.

[36] X.S. Liang, S.Q. Yang, J.G. Li, H. Zhang, Q. Diao, W. Zhao, G.Y. Lu, Mixed-potential-type zirconia-based NO_2 sensor with high-performance three-phase boundary, Sens. Actuators B: Chem. 158 (2011) 1–8.

[37] N. Miura, G.Y. Lu, N. Yamazoe, Progress in mixed-potential type devices based on solid electrolyte for sensing redox gases, Solid State Ionics 136–137 (2000) 533–542.

[38] N. Miura, H. Kurosawa, M. Hasei, G.Y. Lu, N. Yamazoea, Stabilized zirconia-based sensor using oxide electrode for detection of NO_x in high-temperature combustion-exhausts, Solid State Ionics 86–88 (1996) 1069–1073.

[39] G.Y. Lu, Q. Diao, C.G. Yin, S.Q. Yang, Y.Z. Guan, X.Y. Cheng, X.S. Liang, High performance mixed-potential type NO_x sensor based on stabilized zirconia and oxide electrode, Solid State Ionics 262 (2014) 292–297.

[40] X.S. Liang, T.G. Zhong, H.S. Guan, F.M. Liu, G.Y. Lu, B.F. Quan, Ammonia sensor based on NASICON and Cr_2O_3 electrode, Sens. Actuators B: Chem. 136 (2009) 479–483.

[41] V. Srivastava, K. Jain, Highly sensitive NH_3 sensor using Pt catalyzed silica coating over WO_3 thick films, Sens. Actuators B 133 (2008) 46–52.

[42] S.K. Biswas, P. Pramanik, Studies on the gas sensing behaviour of nanosized $CuNb_2O_6$ towards ammonia, hydrogen and liquefied petroleum gas, Sens. Actuators B 133 (2008) 449–455.

[43] A. Satsuma, M. Katagiri, S. Kakimoto, S. Sugaya, K. Shimizu, Effects of calcination temperature and acid–base properties on mixed potential ammonia sensors modified by metal oxides, Sensors 11 (2011) 2155–2165.

[44] D.Y. Wang, S. Yao, M. Shost, J. Yoo, D. Cabush, D. Racine, R. Cloudt, F. Willems, Ammonia sensor for closed-loop SCR control, SAE Int. J. Passeng. Cars Electron. Electr. Syst. (2009) 323–333, http://dx.doi.org/10.4271/2008-01-0919, ISSN: 1946-4614.

[45] S. Zhuiykow, N. Miura, Development of zirconia-based potentiometric NO_x sensors for automotive and energy industries in the early 21st century: what are the prospects for sensors, Sens. Actuators B: Chem. 121 (2007) 639–651.

[46] P. Elumalai, J. Wang, S. Zhuiykov, N. Miura, Sensing characteristics of YSZ-based mixed-potential-type planar NO_x sensors using NiO sensing electrodes sintered at different temperatures, J. Electrochem. Soc. 152 (2005) H95–H101.

[47] N. Miura, Y. Yan, G.Y. Lu, N. Yamazoe, Sensing characteristics and mechanism of hydrogen sulfide sensor using stabilized zirconia and oxide sensing electrode, Sens. Actuators B: Chem. 34 (1996) 367–371.

[48] N. Miura, T. Raisen, G.Y. Lu, N. Yamazoe, Highly selective CO sensor using stabilized zirconia and a couple of oxide electrodes, Sens. Actuators B: Chem. 47 (1998) 84–91.

[49] Y.Z. Guan, C.G. Yin, X.Y. Cheng, X.S. Liang, Q. Diao, H. Zhang, G.Y. Lu, Sub-ppm H_2S sensor based on YSZ and hollow balls $NiMn_2O_4$ sensing electrode, Sens. Actuators B: Chem. 193 (2014) 501–508.

Biographies

Fangmeng Liu received his B.S. degree in 2009 from College of Chemistry, Liaocheng University and M.S. degree in 2012 from Northeast Forestry University in China. Currently he is studying for his Ph.D. degree in College of Electronic Science and Engineering, Jilin University, China.

Ruize Sun received the B.Eng. degree in Department of Electronic Science and Technology in 2012. He is currently studying for his M.E.Sci. degree in College of Electronic Science and Engineering, Jilin University, China.

Yehui Guan received the B.Eng. degree in department of electronic science and technology in 2014. He is currently studying for his M.E.Sci. degree in College of Electronic Science and Engineering, Jilin University, China.

Xiaoyang Cheng received the B.Sci. degree in Department of Electronic Science and Technology in 2013. She is study for her M.E.Sci. degree in College of Electronic Sciences and Technology, Jilin University, China. Her current research is solid electrolyte gas sensor.

Han Zhang received the B.Eng. degree in Department of Electronic Sciences and Technology in 2009. He is currently studying for his M.E.Sci. degree in College of Electronic Science and Engineering, Jilin University, China.

Yingzhou Guan received the B.Eng. degree in Department of Electronic Sciences and Technology in 2012. He is currently studying for his M.E.Sci. degree in College of Electronic Science and Engineering, Jilin University, China.

Xishuang Liang received the B.Eng. degree in Department of Electronic Science and Technology in 2004. He received his Doctor's degree in College of Electronic Science and Engineering at Jilin University in 2009. Now he is an associate professor of Jilin University, China. His current research is solid electrolyte gas sensor.

Peng Sun received his Ph.D. degree from the Electronics Science and Engineering Department, Jilin University, China in 2014. Now, he is engaged in the synthesis and characterization of the semiconducting functional materials and gas sensors.

Geyu Lu received the B.Sci. degree in electronic sciences in 1985 and the M.S. degree in 1988 from Jilin University in China and the Dr. Eng. degree in 1998 from Kyushu University in Japan. Now he is a professor of Jilin University, China. His current research interests include the development of chemical sensors and the application of the function materials.